Pseudorapidity distributions of charged particles as a function of centrality in Pb-Pb collisions at 158 and 40 GeV per nucleon incident energy

M.C. Abreu, B. Alessandro, C. Alexa, R. Arnaldi, M. Atayan, C. Baglin, A. Baldit, M. Bedjidian, S. Beole, V. Boldea, et al.

Pseudorapidity distributions of charged particles as a function of centrality in Pb–Pb collisions at 158 and 40 GeV per nucleon incident energy

NA50 collaboration

M.C. Abreu[7,a], B. Alessandro[12], C. Alexa[4], R. Arnaldi[12], M. Atayan[14], C. Baglin[2], A. Baldit[3], M. Bedjidian[13], S. Beolè[12], V. Boldea[4], P. Bordalo[7,b], G. Borges[7], A. Bussière[2], L. Capelli[13], C. Castanier[3], J. Castor[3], B. Chaurand[10], I. Chevrot[3], B. Cheynis[13], E. Chiavassa[12], C. Cicalò[5], T. Claudino[7], M.P. Comets[9], N. Constans[10], S. Constantinescu[4], P. Cortese[1] A. De Falco[5], N. De Marco[12], G. Dellacasa[1], A. Devaux[3], S. Dita[4], O. Drapier[10], L. Ducroux[13], B. Espagnon[3], J. Fargeix[3], P. Force[3], M. Gallio[12], Y.K. Gavrilov[8], C. Gerschel[9], P. Giubellino[12,c], M.B. Golubeva[8], M. Gonin[10], A.A. Grigorian[14], S. Grigorian[14], J.Y. Grossiord[13], F.F. Guber[8], A. Guichard[13], H. Gulkanyan[14], R. Hakobyan[14], R. Haroutunian[13], M. Idzik[12,d], D. Jouan[9], T.L. Karavitcheva[8], L. Kluberg[10], A.B. Kurepin[8], Y. Le Bornec[9], C. Lourenço[6], P. Macciotta[5], M. Mac Cormick[9], A. Marzari-Chiesa[12], M. Masera[12,c], A. Masoni[5], M. Monteno[12], A. Musso[12], P. Petiau[10], A. Piccotti[12], J.R. Pizzi[13], W.L. Prado da Silva[12,e], F. Prino[12], G. Puddu[5], C. Quintans[7], L. Ramello[1], S. Ramos[7,b], P. Rato Mendes[7], L. Riccati[12], A. Romana[10], H. Santos[7], P. Saturnini[3], E. Scalas[1] E. Scomparin[12], S. Serci[5], R. Shahoyan[7,f], F. Sigaudo[12], S. Silva[7], M. Sitta[1], P. Sonderegger[6,b], X. Tarrago[9], N.S. Topilskaya[8], G.L. Usai[5,c], E. Vercellin[12], L. Villatte[9], N. Willis[9].

Abstract

The charged particle distributions $dN_{ch}/d\eta$ have been measured by the NA50 experiment in Pb–Pb collisions at the CERN SPS. Measurements have been done at incident energies of 158 and 40 GeV per nucleon over a broad impact parameter range. Results obtained with two independent centrality estimators, namely the neutral transverse energy E_T and the forward energy E_{ZDC}, are reported.

[1] Università del Piemonte Orientale, Alessandria and INFN-Torino, Italy

[2] LAPP, CNRS-IN2P3, Annecy-le-Vieux, France.

[3] LPC, Univ. Blaise Pascal and CNRS-IN2P3, Aubière, France.

[4] IFA, Bucharest, Romania.

[5] Università di Cagliari/INFN, Cagliari, Italy.

[6] CERN, Geneva, Switzerland.

[7] LIP, Lisbon, Portugal.

[8] INR, Moscow, Russia.

[9] IPN, Univ. de Paris-Sud and CNRS-IN2P3, Orsay, France.

[10] LPNHE, Ecole Polytechnique and CNRS-IN2P3, Palaiseau, France.

[11] IRS, Univ. Louis Pasteur and CNRS-IN2P3, Strasbourg, France.

[12] Università di Torino/INFN, Torino, Italy.

[13] IPN, Univ. Claude Bernard and CNRS-IN2P3, Villeurbanne, France.

[14] YerPhI, Yerevan, Armenia.

[a] also at FCT, Universidade de Algarve, Faro, Portugal

[b] also at IST, Universidade Técnica de Lisboa, Lisbon, Portugal

[c] also at CERN, Geneva, Switzerland

[d] also at Faculty of Physics and Nuclear Techniques, University of Mining and Metallurgy, Cracow, Poland

[e] now at UERJ, Rio de Janeiro, Brazil

[f] on leave of absence from YerPhI, Yerevan, Armenia

1   Introduction

Heavy ion collisions at ultra–relativistic energies are a powerful tool to study nuclear matter under conditions of very high density and temperature. The multiplicity of charged particles produced in the collisions is a global variable that is essential for their characterization, because it quantifies to which extent the incoming beam energy is released to produce new particles. The multiplicity detector of the NA50 experiment, with its good granularity, allows to measure the charged particle multiplicity as a function of pseudorapidity, providing in particular the particle density at midrapidity. This observable gives information about initial conditions such as the energy density, whose knowledge is relevant for the interpretation of the anomalous J/ψ suppression, observed by the NA50 experiment in Pb-Pb collisions [1, 2, 3], in terms of the threshold for the creation of a new state of matter.

The pseudorapidity distributions of primary charged particles are presented in this paper for different classes of events selected according to the centrality of the collision. Two analyses have been performed using two independent centrality-related observables: the energy of the projectile spectator nucleons measured by a Zero Degree Calorimeter and the neutral transverse energy measured by an Electromagnetic Calorimeter. In both cases, the centrality selection has been made using observables which are independent of the multiplicity detector itself, in order to avoid autocorrelations. Preliminary results were reported in [4].

2   Apparatus and data taking conditions

The NA50 apparatus consists of a muon spectrometer equipped with three detectors which measure global observables on an event-by-event basis (namely charged particle multiplicity, neutral transverse energy and forward energy) and specific devices for beam tagging and interaction vertex identification. The complete detector setup has been presented elsewhere [5]. Here we give some details only on the detectors relevant for the present analysis, as shown in Fig. 1.

The multiplicity measurement is done with a silicon strip Multiplicity Detector (MD) [6, 7, 8]. The MD is composed of two identical detector planes called MD1 and MD2, located 10 cm apart. Each of them is a disc of inner radius 6.5 mm and outer radius 88.5 mm (sensitive part), segmented azimuthally in 36 sectors of $\Delta\phi = 10°$ and radially in 192 strips with different sizes in order to have almost constant occupancy per strip. Only digital (hit/no hit) information is provided for each strip. The average granularity is $\Delta\eta \simeq 0.02$. The two planes cover the full 2π azimuth, while the nominal η ranges covered are 1.11< η <3.51 for MD1 and 1.61< η <4.13 for MD2, for a target located at 11.65 cm from the center of MD1. Since for the analysis presented in this paper only the 128 innermost strips have been used, the η coverage is restricted to 1.93< η <3.51 and 2.47< η <4.13 for MD1 and MD2 respectively.

The determination of the centrality of the collision is obtained by means of two different detectors. The Zero Degree Calorimeter (ZDC) [9], made of quartz fibers
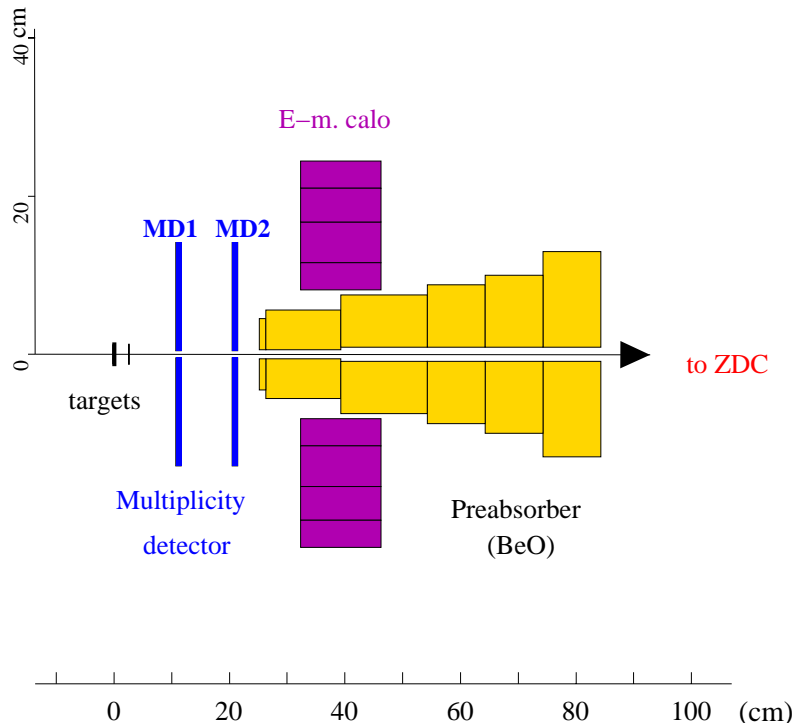
Figure 1: 1998 experimental setup.

embedded in tantalum, positioned on the beam axis inside the hadron absorber of the spectrometer, measures the energy E_{ZDC} of the spectator nucleons travelling in the forward direction, i.e. in the range $\eta \geq 6.3$. The second centrality detector is an electromagnetic calorimeter (EMCAL) made of scintillating fibers embedded into a 14 cm thick lead converter, which measures the neutral transverse energy E_T in the pseudorapidity domain $1.1 < \eta < 2.3$.

The main triggers of the experiment are the dimuon trigger [5] and, more relevant for this analysis, the minimum bias trigger provided by the Zero Degree Calorimeter, generated every time a minimum amount of energy is released in the ZDC. Even for the most central collisions, a few particles produced in the ZDC angular acceptance provide a signal.

Data collected at two different energies of the SPS Pb beam have been used for this analysis: the first data sample was taken in 1998 at 158 GeV per nucleon incident energy, corresponding to $\sqrt{s} = 17.3$ GeV, the second in 1999 at 40 GeV/nucleon energy ($\sqrt{s} = 8.77$ GeV). Special runs taken with the minimum bias trigger at low beam intensity (about 1/10 of the standard intensity used by the experiment) have been used. The average Pb beam intensity, the thickness and the position of the targets are listed in table 1.

Beam energy (GeV/nucleon)	Beam intensity (ions/5 s burst)	Target thickness	Distance (cm) target-MD1	# of events analyzed
158	$3.2 \cdot 10^6$	3 mm	11.65	48000
158	$3.9 \cdot 10^6$	1 mm	9.15	18000
40	$1 \cdot 10^6$	3 mm	12.55	35000

Table 1: Data taking conditions.

3 Centrality selection

The aim of our analysis is to study the properties of $dN_{ch}/d\eta$ distributions in Pb–Pb collisions as a function of centrality using two independent centrality estimators, namely the forward energy E_{ZDC} and the transverse energy E_T. To allow a comparison of the results obtained with these two different variables, centrality intervals have been defined in terms of fractions of the inelastic cross section which was calculated by integrating the Minimum Bias (MB) dN/dE_{ZDC} and dN/dE_T distributions.

Since the MB spectra contain also events from non-interacting Pb projectiles, to obtain the number of interactions (N_{int}), the integral of the MB spectra N_{Pb} has to be normalized taking into account the interaction probability P_{int}:

$$N_{int} = N_{Pb} \cdot P_{int} = N_{Pb} \cdot \left(1 - e^{-L_T/\lambda_{int}}\right)$$

where L_T is the target thickness (see table 1) and λ_{int} is the interaction length, which can be expressed as:

$$\lambda_{int} = \frac{A_{targ}}{\rho_{Pb} \cdot N_A \sigma_{inel}}$$

where $A_{targ} = 207.2$ is the atomic mass of the target (Pb) nucleus, N_A is the Avogadro number, $\rho_{Pb} = 11.35$ g/cm^3 and σ_{inel} is the total inelastic cross section, given by:

$$\sigma_{inel} = \sigma_0 (A_{proj}^{1/3} + A_{targ}^{1/3} - \delta)^2$$

Assuming $\sigma_0 = 68.8$ mb and $\delta = 1.32$ (obtained interpolating from the values given in [10, 11]) one obtains:

$$\sigma_{inel} = 7.62^{+0.54}_{-1.23} \text{ b} \qquad \lambda_{int} = 3.98^{+0.21}_{-0.27} \text{ cm} \qquad P_{int}(L_T = 3 \text{ mm}) = 7.26^{+0.51}_{-0.35} \cdot 10^{-2}$$

3.1 Data at 158 GeV/nucleon

The E_{ZDC} and E_T distributions of MB events at 158 GeV/nucleon beam energy are shown in fig. 2. The limits of each centrality class have been fixed so as to have classes with a width corresponding to 5% of the total inelastic cross section σ_{inel}. When the 5% class would have been too narrow with respect to the E_{ZDC} or E_T resolution giving thus rise to possible biases in the centrality selection, a class with a

width corresponding to $10\% \cdot \sigma_{inel}$ has been defined. In this way, 6 centrality classes have been defined for both centrality estimators. The E_{ZDC} and E_T limits for the different centrality classes are plotted in fig. 2 and are listed in table 2 together with the mean E_{ZDC} and E_T value for each class.
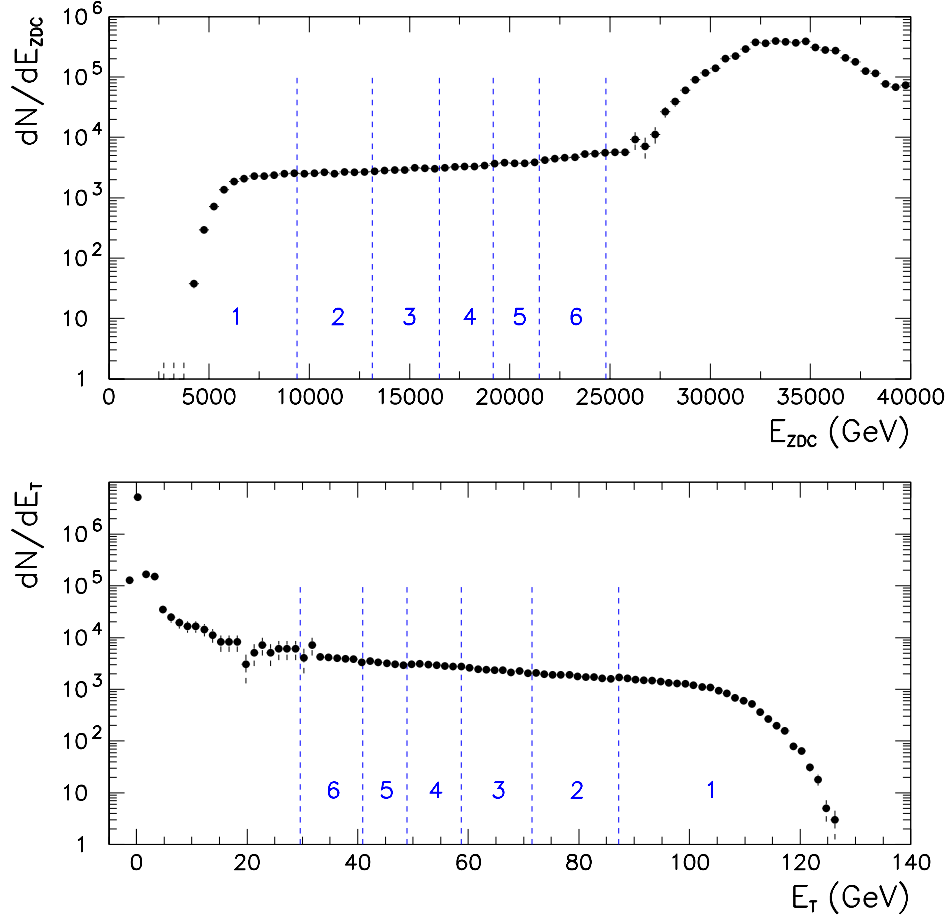
Figure 2: Distributions of the forward energy E_{ZDC} and of the transverse energy E_T in 158·A GeV/c Pb–Pb Minimum Bias collisions.

The $\simeq 5\%$ uncertainty on the value of P_{int} is reflected in a $\simeq 5\%$ uncertainty in the evaluation of the total inelastic cross section fraction. This corresponds to uncertainties of $\sim 300 - 500$ GeV on the E_{ZDC} limits of each class and $\sim 2 - 3$ GeV on the E_T limits, which give the systematic errors on $< E_{ZDC} >$ and $< E_T >$ quoted in table 2.

CLASS	% of c.s.	E_{ZDC}^{min}-E_{ZDC}^{max} (GeV)	$< E_{ZDC} >$ (GeV)	Syst. err. $< E_{ZDC} >$ (GeV)
1	0-5	0-9385	7500	130
2	5-10	9385-13150	11280	380
3	10-15	13150-16490	14790	620
4	15-20	16490-19180	17790	770
5	20-25	19180-21475	20250	650
6	25-35	21475-24790	23110	650

CLASS	% of c.s.	E_T^{min}-E_T^{max} (GeV)	$< E_T >$ (GeV)	Syst. err. $< E_T >$ (GeV)
1	0-5	87.2-140.	98.3	1
2	5-10	71.5-87.2	78.6	2
3	10-15	58.7-71.5	64.5	2
4	15-20	48.9-58.7	53.4	2
5	20-25	40.9-48.9	44.4	2
6	25-35	29.6-40.9	34.9	2

Table 2: E_{ZDC} and E_T limits for the different centrality classes at 158 GeV/nucleon.

3.2   Data at 40 GeV/nucleon

The same method has been applied to the data sample collected in 1999 at 40 GeV per nucleon incident energy. Due to the worse performance of the ZDC at such a low beam energy, it was not possible to use both centrality estimators and only the analysis with the E_T based centrality selection has been performed. The E_T spectrum of Minimum Bias events is shown in fig. 3. The limits of the centrality classes (indicated by vertical bars on the spectrum in fig. 3) correspond to the same intervals of total inelastic cross-section fraction used for the 158 GeV/nucleon data sample. Their numerical values can be found in the legend of fig. 8. At this energy, a larger uncertainty on the centrality intervals is expected as a consequence of the worse resolution of the electromagnetic calorimeter with respect to the 158 GeV/nucleon data sample. Moreover the unavailability of the ZDC information does not allow to make a cross-check with an independent centrality estimator. This affects in particular the most central interval, whose cross-section fraction limit we estimate to be $5^{+1}_{-0.5}\%$.

4   Event analysis

The data analysis has been performed both in the centrality classes defined by E_T and in the ones defined by E_{ZDC}, according to the following procedure. First some quality cuts on the data sample have been applied. Then in each centrality class
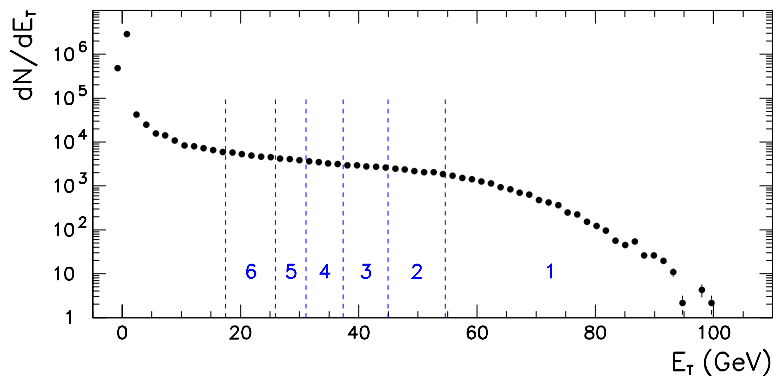
Figure 3: E_T in Pb–Pb collisions at 40 GeV per nucleon incident energy. The limits of the 6 centrality classes are superimposed.

the raw $dN_{ch}/d\eta$ distribution has been calculated. Finally, the primary $dN_{ch}/d\eta$ distribution has been obtained by subtracting the delta electron contribution and then by correcting for secondary processes. Gamma conversions and other processes of secondary particle production or primary particle decay have been evaluated with a complete Monte Carlo simulation based on the VENUS 4.12 [12] event generator and on the GEANT 3.21 [13] package for track propagation and detector response simulation. Below we give some details of the analysis performed for each step. More details can be found in [14].

4.1 Data selection

Events have been selected according to the following criteria. The beam hodoscope recognizes events with two or more ions incident within a 20 ns time window, which could produce pile–up, and are therefore rejected. Interactions occurring upstream from the target are rejected by means of scintillators located close to the beam line. Furthermore, we define as being on–target the events lying in a chosen E_T versus E_{ZDC} correlation band (see e.g. Fig. 1 of [2]). A further constraint on the vertex position has been applied by requiring the correct geometrical correlation between the hits in the two multiplicity detector planes (MD1, MD2) [1].

4.2 Raw multiplicity evaluation

The main difficulty in the extraction of the particle multiplicity from the observed detector occupancy is connected to the presence of many strip clusters, i.e. groups of 2 or more contiguous detector strips firing at the same time.

---

[1]We have verified that this selection (not applied in fig. 2 and 3) does not affect our centrality classes except for a slight reduction of the number of events in the most peripheral E_{ZDC} class ($21475 < E_{ZDC} < 24790$).

The origin of clusters could be both physical and instrumental. The physical cluster mechanism is due to particles crossing contiguous strips and to the effects of particle energy deposition inside the detector. By instrumental origin we refer to all clustering sources connected to a deteriorated performance of the detector and front–end electronics. Considering a real system performance, one of the most likely candidates for instrumental clustering effect is the crosstalk between channels in the front–end electronics system. The crosstalk effect gives rise to clustering effects similar to the ones coming from physical processes. Systems having significant crosstalk would show a cluster distribution shifted towards bigger cluster sizes.

Since a VENUS+GEANT Monte Carlo simulation of the full detector system, which includes only clusters of physical origin, does not reproduce the cluster distributions observed in the experimental data, a correction to account for clusters of instrumental origin is needed. The method used to get the true particle occupancy from the measured strip occupancy is based on minimization techniques aimed at reproducing the cluster distribution of the experimental data.

The strip occupancy is simulated generating the particle distributions in the detector and afterwards including the effects responsible for clustering. The particles are generated in each pseudorapidity bin according to a Poissonian distribution whose mean equals the particle occupancy. The clustering mechanisms are modeled by means of coefficients describing the probability that the strips in the vicinity of real particle tracks are firing. Then for a given particle occupancy and probability coefficients, the cluster distribution is calculated and compared to the observed one. This procedure is applied iteratively, changing the particle occupancy and the probability coefficients, until the generated cluster distribution reproduces the experimental one. The particle occupancy per strip obtained in this way is then used to calculate the raw $dN_{ch}/d\eta$ distributions, taking into account the geometrical acceptance of the strips in each η bin.

The stability of reconstructed particle occupancies against the initial values of the parameters has been checked. For testing purposes the method has been applied to VENUS+GEANT generated data in the complete detector system for different centrality classes. It has been found that the reconstructed $dN_{ch}/d\eta$ distributions are in agreement with the generated ones within 5%. For experimental data samples we checked that in each centrality class the reconstructed occupancy for a given pseudorapidity bin agrees within 6% among adjacent azimuthal sectors of the detector. The ratio between the observed detector occupancy and the real particle occupancy ranges from ~ 1 for peripheral (low multiplicity) events to ~ 1.8 for central (high multiplicity) events.

4.3   Primary particle multiplicity evaluation

The δ ray contribution to the detector occupancy is evaluated by means of a GEANT 3.21 simulation, taking into account the effects of the target and of all the other materials, including the mechanical support of the detectors. This contribution reaches

a maximum of 5% of the true occupancy, in the most peripheral sample considered in this paper.

The VENUS+GEANT $dN_{ch}/d\eta$ distributions for different centrality classes are reconstructed with the same method as the one used for the experimental data. This is done in order to keep exactly the same treatment for experimental and Monte Carlo data, so that possible systematics are canceled. The secondary/primary correction factors are obtained dividing VENUS+GEANT reconstructed $dN_{ch}/d\eta$ distributions by the primary VENUS $dN_{ch}/d\eta$ distributions. We have run VENUS 4.12 with the default setting for decays of unstable particles, except for neutral pions (whose decay has been taken in charge by GEANT), meaning that charged particles from decays of K_0's, Λ's and other hyperons are considered as primary. The correction factors range from 1.2 to 1.8 depending on target thickness, on target position and on the particular multiplicity detector plane. The primary experimental $dN_{ch}/d\eta$ distributions are obtained dividing the raw $dN_{ch}/d\eta$ distributions, after δ subtraction, by the secondary/primary correction factors.
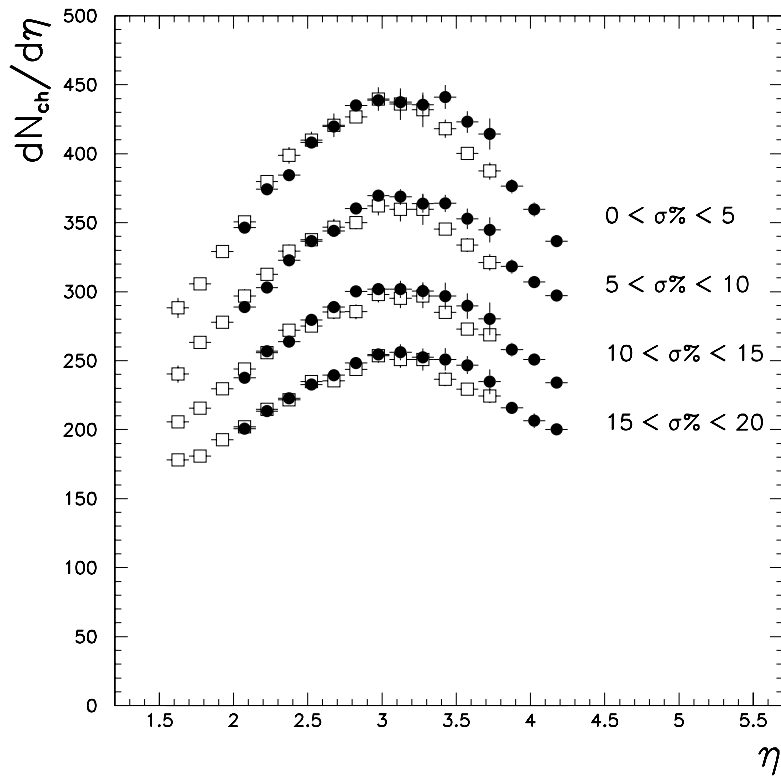

Figure 4: Comparison of corrected pseudorapidity distributions for the 1 mm (open squares) and the 3 mm (closed circles) targets; the two targets were placed 2.5 cm apart and lead to different η regions covered by MD.

8

The resulting $dN_{ch}/d\eta$ particle distributions from MD1 and MD2, being in agreement in their common η range, are then merged together, providing a wider η coverage. As a final check, the complete procedure is applied to two data samples with different target thickness and position: the results agree, as shown in Fig. 4.

Including other error sources not discussed so far, as uncertainties on the discrimination threshold of the front-end electronics channels, possible misalignments of the detectors and influence of the primary particle composition (depending on the VENUS model) on the Monte Carlo secondary/primary correction factor, we estimate the overall systematic error on the evaluated multiplicity to be below 8%. For the 40 GeV/nucleon data, since only one centrality estimator is used, a larger systematic error (10%) is estimated.

5   Experimental results

5.1   Results at 158 GeV/nucleon

The pseudorapidity distributions of charged particles obtained using E_{ZDC} and E_T as centrality estimators (see table 2) are shown respectively in fig. 5 and in fig. 6. The pseudorapidity coverage is approximately centered at midrapidity and extends over ~ 2.2 units, so that the $dN_{ch}/d\eta$ peak is visible in the pseudorapidity distributions without any reflection around midrapidity. The $dN_{ch}/d\eta$ distributions are rather symmetrical around the midrapidity point ($\eta_{max} \simeq 3.1$ corresponding [2] to y_{max}=2.91) and their heights increase steadily with increasing centrality.

The $dN_{ch}/d\eta$ distributions have been integrated in the range $2.45 < \eta < 3.65$ (approximately symmetric around midrapidity) and divided by the width of the pseudorapidity interval considered ($\Delta\eta = 1.2$), to obtain the average value of the charged particle pseudorapidity density at midrapidity ($< dN_{ch}/d\eta >|_{mid}$).

Depending on the variable (E_T or E_{ZDC}) used as centrality estimator, two different values of $< dN_{ch}/d\eta >|_{mid}$ have been obtained. The relative difference between these two estimations amounts to $\simeq 1.5\%$ for the five most central classes, while for the most peripheral class it is below 3%.

In fig. 7 the value of $< dN_{ch}/d\eta >|_{mid}$ as a function of centrality is plotted, showing an approximately linear dependence of the charged multiplicity on both E_T and E_{ZDC}. The average value of charged particle pseudorapidity density for the most central class of events (0-5% of the total inelastic cross-section) is:

$$< dN_{ch}/d\eta >|_{mid} = 428 \pm 1(stat) \pm 34(syst)$$

averaged over the values obtained using E_{ZDC} and E_T as centrality estimators. This result can be compared with the corresponding one extracted from a VENUS 4.12 simulation, which is:

$$< dN_{ch}/d\eta^{VENUS} >|_{mid} = 465 \pm 6.$$

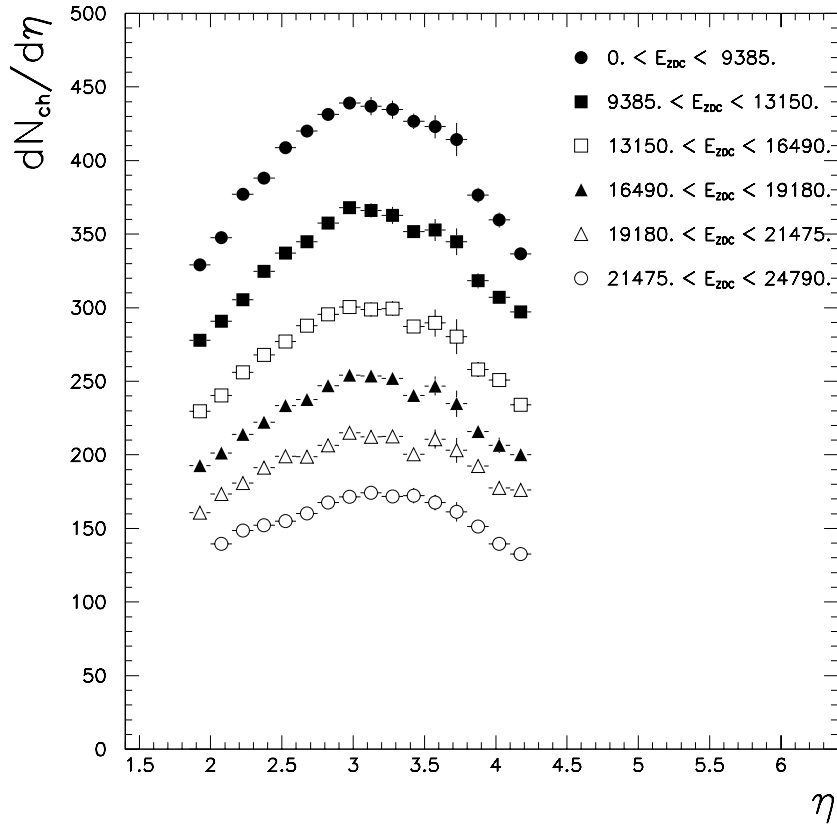[2]The shift of $\approx$0.2 units between y_{max} and η_{max} has been extracted from VENUS.

Figure 5: $dN_{ch}/d\eta$ distributions at 158 GeV per nucleon, obtained using E_{ZDC} as centrality estimator. The 8% systematic error on the multiplicity evaluation is not included in the data points.
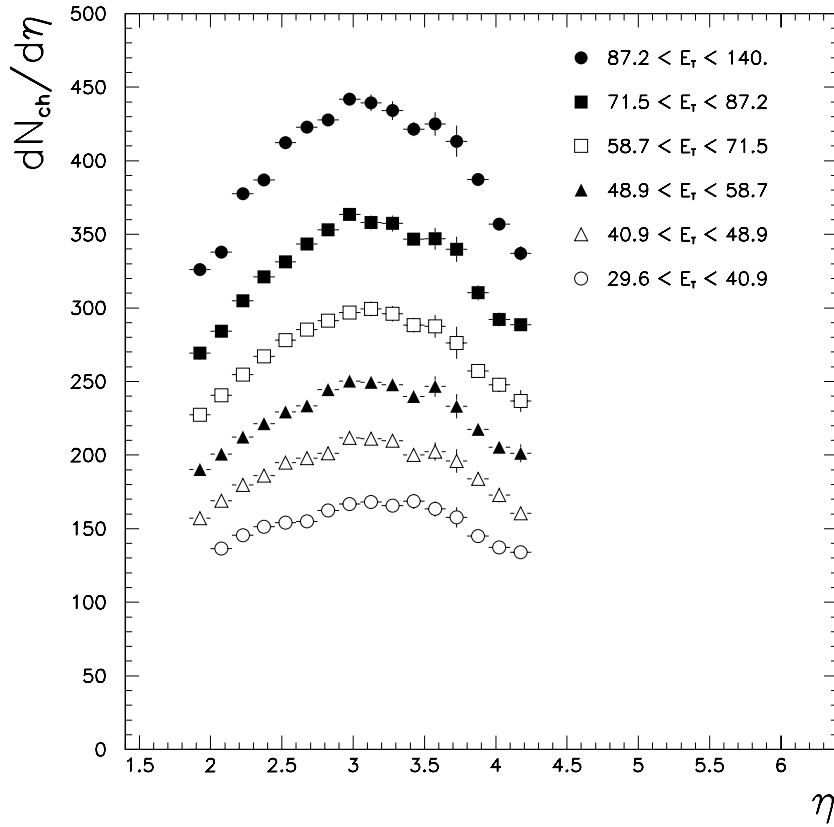
Figure 6: $dN_{ch}/d\eta$ distributions at 158 GeV per nucleon, obtained using E_T as centrality estimator (8% systematic error not included).
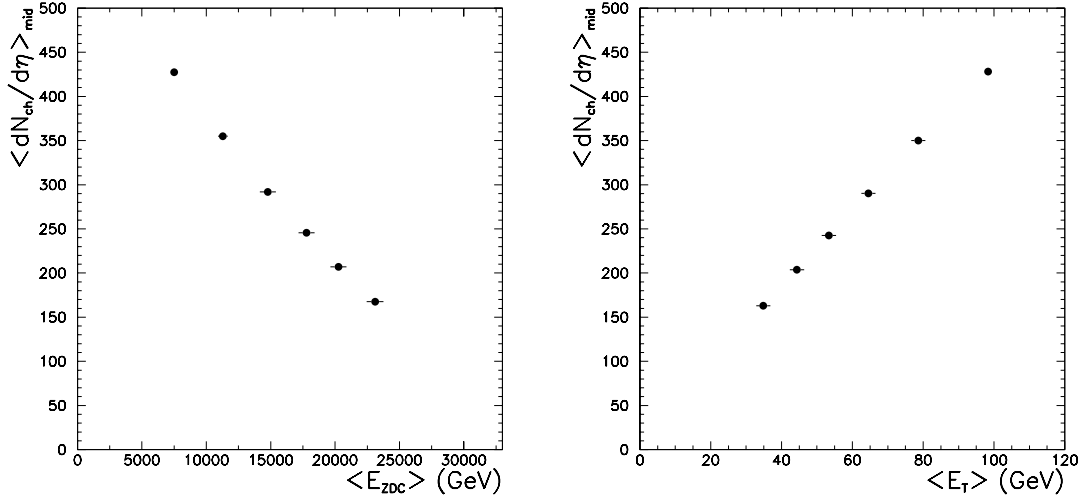
Figure 7: Average charged particle pseudorapidity density at midrapidity as a function of E_{ZDC} (left panel) and E_T (right panel). The 8% systematic error on the charged multiplicity evaluation is not included. The statistical error bars on $< dN_{ch}/d\eta >|_{mid}$ are smaller than the symbol sizes.

and turns out to be 8% higher than our measured value.

The average primary charged multiplicity in the pseudorapidity range $2.75 < \eta < 3.95$ (approximately equal to the muon spectrometer acceptance) has been calculated by integrating the $dN_{ch}/d\eta$ distributions, obtaining for the 5% most central events:

$$< N_{ch} >|_{2.75<\eta<3.95} = 508 \pm 2(stat) \pm 40(syst)$$

5.2   Results at 40 GeV/nucleon

The same analysis has been performed on data collected at 40 GeV per nucleon beam energy. The $dN_{ch}/d\eta$ distributions are shown in fig. 8.

The average value of the charged particle pseudorapidity density at midrapidity has been evaluated over the interval $2.15 < \eta < 2.90$, approximately symmetric around the midrapidity value $\eta_{max} \approx 2.47$, extracted from VENUS. It scales linearly as a function of E_T, as it can be seen in fig. 9. For the most central class (0-5% of the total inelastic cross-section) it is:

$$< dN_{ch}/d\eta >|_{mid} = 207 \pm 1(stat) \pm 16(syst)$$

approximately 2 times smaller than the value measured at 158 GeV per nucleon.
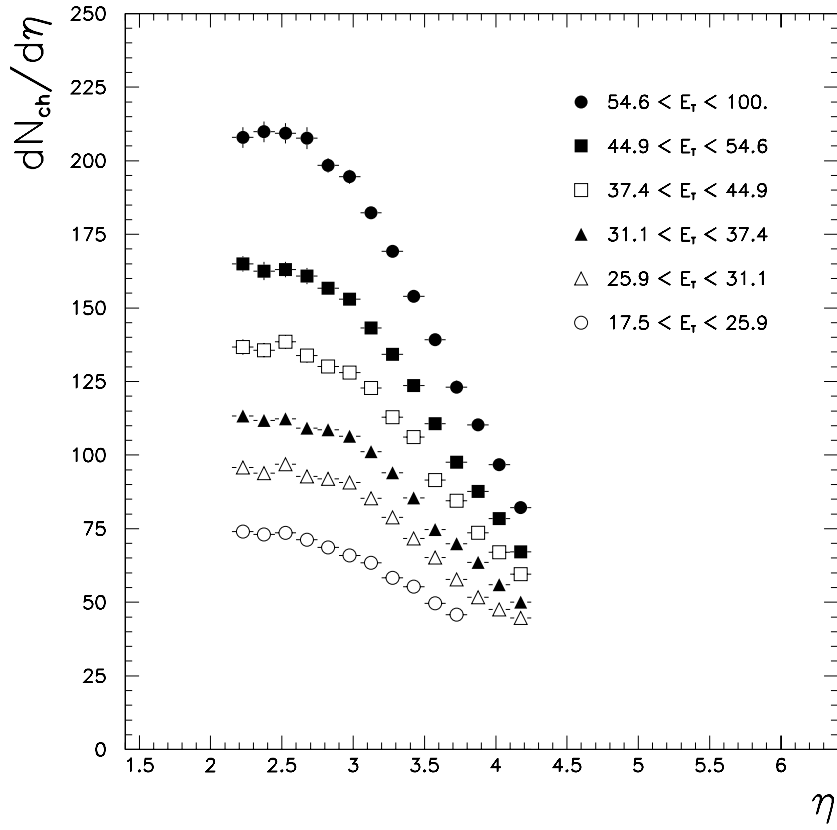
12

Figure 8: $dN_{ch}/d\eta$ distributions at 40 GeV per nucleon, obtained using E_T as centrality estimator (10% systematic error not included in the data points).
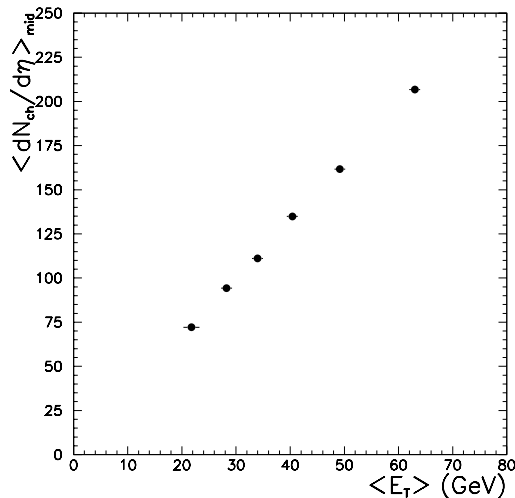
Figure 9: Average charged particle pseudorapidity density at midrapidity as a function of E_T for Pb-Pb collisions at 40 GeV per nucleon incident energy. The 10% systematic error on the charged multiplicity evaluation is not included. The statistical error bars on $< dN_{ch}/d\eta >|_{mid}$ are smaller than the symbol sizes.

6   Conclusions

The charged particle pseudorapidity distributions $(dN_{ch}/d\eta)$ in Pb-Pb collisions at 158 GeV per nucleon ($\sqrt{s}$=17.3 GeV) and 40 GeV per nucleon ($\sqrt{s}$=8.77 GeV) beam energy have been measured in 6 centrality classes defined in terms of fractions of the total inelastic cross-section.

Data at 158 GeV/nucleon have been analyzed using two independent centrality estimators, namely the forward energy E_{ZDC} and the neutral transverse energy E_T. The results obtained are in agreement within $\simeq 1.5\%$ for the four most central classes of events and within 3% for the most peripheral events considered in this analysis.

The average charged particle pseudorapidity density in a η interval symmetric around the peak has been evaluated for each centrality class and shows an approximately linear correlation with both measured centrality-related variables (E_{ZDC} and E_T). No saturation or enhancement of the charged multiplicity is observed up to the most central E_T or E_{ZDC} interval considered in this analysis. This conclusion is also valid for the 40 GeV per nucleon data sample for which only the analysis in terms of E_T has been performed.

From the comparison of the data collected at the two energies it results that the charged multiplicity increases by a factor of $\simeq 2$ when going from $\sqrt{s}$=8.77 GeV to $\sqrt{s}$=17.3 GeV.

A further analysis of these results as a function of the number of participant nucleons and of the number of binary nucleon-nucleon collisions is presented in [15].

Acknowledgements

References

[1] M.C. Abreu et al., NA50 Collaboration, *Phys.Lett.* **B 410** (1997) 337.

[2] M.C. Abreu et al., NA50 Collaboration, *Phys.Lett.* **B 450** (1999) 456.

[3] M.C. Abreu et al., NA50 Collaboration, *Phys.Lett.* **B 477** (2000) 28.

[4] M. Idzik et al., NA50 collaboration, Proc. of the 29th Int. Symposium on Multiparticle Dynamics: QCD and Multiparticle Production, World Scientific, Singapore 2000.

[5] M.C. Abreu et al., NA50 Collaboration, *Phys.Lett.* **B 410** (1997) 327.

[6] B. Alessandro et al., *Nucl.Inst.Meth.* **A 360** (1995) 189.

[7] B. Alessandro et al., *Nucl.Inst.Meth.* **A 432** (1999) 342.

[8] B. Alessandro et al., The silicon Multiplicity Detector for the NA50 experiment at CERN, in preparation.

[9] R. Arnaldi et al., *Nucl.Inst.Meth.* **A 411** (1998) 1.

[10] H. Dekhissi et al., *Nucl. Phys.* **A 662** (2000) 207.

[11] E. Andersen et al., NA36 Collaboration, *Phys. Lett.* **B 220** (1989) 328.

[12] K. Werner, *Phys. Rep.***232** (1993) 87.

[13] R. Brun et al., GEANT3, CERN/DD/cc/84-1.

[14] F. Prino, Ph.D. thesis, University of Torino, Dec. 2001.

[15] M.C. Abreu et al., NA50 Collaboration, Scaling of charged particle multiplicity in Pb-Pb collisions at SPS energies, submitted to Phys. Lett.